Thermal Stability of Epoxy Nanocomposites: Surface Treatment and Morphology Impact Based on Nano SiO₂ and hBN Fillers

Dayuan Qiang[1,2], Xinyu Wang[1,2], Yan Wang[3], Thomas Andritsch[1,2] and George Chen[1,2]

[1] School of Electronic and Computer Science, University of Southampton, Southampton, United Kingdom
[2] The Tony Davies High Voltage Laboratory, University of Southampton, Southampton, United Kingdom
[3] Complex lab, College of Computer Science and Engineering, University of Electronics Science and Technology of China, Chengdu, China

E-mail: opstraxex@gmail.com

Abstract

Epoxy resin is one of the most commonly used thermosetting macromolecular synthetic materials. It displays excellent adhesiveness properties, good dielectric property, mechanical property and chemical stability. Consequently, epoxy resins have been widely used for many industrial purposes, such as electrical casting into power transformers, ignition coil systems and potting. In this paper, TGA and DSC measurements were carried out to evaluate the thermal stability of epoxy nanocomposites. Based on the results of dispersion and distribution of particles within epoxy nanocomposites, it concluded that both presences of nano SiO₂ and hexagonal BN (hBN) particles have obvious impact on base materials in which the influences of latter particle are much more significant due to its shape, and thus both fillers leads to worse thermal stability than pure samples. However, particles could act as flame retardants in polymer nanocomposites and postpone the initiation of decomposition by hindering/slowing the oxidisation. When compared within two SiO₂ based nanocomposites, the surface treatment seems to help mitigate the influences on base materials by achieving better filler dispersion and modify the cross-linking density at the interfacial areas by removing surface functional groups.

Keywords: thermal stability, epoxy nanocomposites, silica, boron nitride, surface treatment, morphology

1. Introduction

Epoxy resin generally refers to epoxy polymers containing two or more epoxy groups and is one of the most commonly used thermosetting macromolecular synthetic materials. Since containing reactive epoxy groups, it can react with many curing agents/hardeners and form three dimensional cross-linking network structures. Epoxy resins show excellent adhesiveness properties, good dielectric property, mechanical property and chemical stability [1]. Because of its advantages, such as low cost and easy shaping, epoxy resins have now widely used and becomes the essential materials for some industrial applications including as insulators [2]. As some applications (e.g., power transformers and potting) require higher thermal stability/conductivity than others [3], with

expecting better performance and broader usage demand, it is challenging to meet the growing requirements and much research has been carried out to look for new methods for modification, including adding nano-fillers to produce nanocomposites (NCs) which is one of the most promising ones [4].

Previous research has intensively studied nano-clay based nanocomposites and concluded thermal stability was improved due to the presence of nano-clay in bulk by TGA measurement [5, 6]. *Kumar* et al. then reviewed most introduced nano-particulates and degradation and stability of resultant nanocomposites. They concluded the presence of nano-fillers undoubtedly enhanced the thermal properties and it was worth doing further studies [7]. *Tarrío-Saavedra* et al. studied the effect of fumed silica on thermal stability of epoxy composites by using three temperature indexes (initial decomposition temperature, maximum rate loss temperature and integral procedure decomposition temperature) in TGA measurement, and finally concluded introduced particles would act as flame retardants to protect the matrix from thermal degradation [8]. However, fillers also led to the low cross-linking density of epoxy nanocomposites and resulted in worse thermal stability. Moreover, they also pointed out the presence of hydroxyl groups on SiO_2 surface affected and led to worse thermal properties as well. *Luo* et al. introduced an interface designed epoxy nanocomposite systems filled with microcrystalline cellulose fibers (MCFs) [9], in which NCs showed enhanced thermal stability as a consequence of improved cross-linking density and glass transition temperature (T_g). Their work proved the strong interfacial interactions could significantly improve the thermal stability of epoxy NC systems. Boron nitride (BN) acting as modification fillers has also attracted numbers of research [10-12]. BN based nanocomposites showed an increase in thermal conductivity due to the presence of BN fillers [10, 11]. *Yu* et al. investigated effects of interfacial modification on thermal properties of boron nitride (BN) nanoplatelets based epoxy nanocomposites [12]. They found surface treatment could improve the thermal properties of nanocomposites.

However, the influences of surface treatment on thermal properties of SiO_2 filled epoxy NCs and thermal stability of epoxy hBN NCs still lack relatively in-depth research. Therefore, the goal of this paper is, first, to investigate how surface treatment to remove hydroxyl groups on the particle surface would affect thermal properties of epoxy nano-SiO_2 based composites. Second, based on TGA and DSC measurements which are usually solely applied in former studies, an overall and comprehensive understanding how the resulting structures due to the presence of nano-fillers can be given according to the morphology analysis. Last, as SiO_2 and hBN particles are in different shapes, it is also important to investigate how this will influence the morphology of epoxy nanocomposites and further relate to their thermal properties.

2. Experiment Preparation

2.1 Materials

The testing samples were prepared based on bisphenol-A diglycidyl ether (D.E.R. 332, density 1.16 $g·cm^{-3}$) along with polyether amine hardener (Jeffamine D-230, density 0.948 $g·cm^{-3}$) supplied by Huntsman. The fillers used in the study are commercially available untreated SiO_2 and BN fillers provided by Sigma-Aldrich and Momentive respectively. More information is detailed and listed in Table 1. Moreover, trimethoxy (octyl) silane was used as a coupling agent to produce C8-treated nano SiO_2 in order to eliminate the hydroxyl groups on the surface of SiO_2 particles and form relatively hydrophobic and unfunctional surface structures (same preparation method was introduced in [13]). The success of modification has also been proved by TGA as shown in Fig. 1 in which surface-treated SiO_2 shows one more weight-loss stage than the untreated ones. In the process of sample preparation, epoxy and its nanocomposites were cured at 120 ℃ for 4 hours with the ratio between epoxy resin and hardener was 1000:344 [14]. Filler loading ratios of nanoparticles are 0.5, 1, 3 and 5 wt%, and following abbreviations are used while coding the samples: **EP** for epoxy resin, **S** for untreated nano-silica composites, **ST** for treated silica, **B** for boron nitride and the number represents the filler loading. For example, EPS1 represents epoxy nanocomposites loaded with 1 wt% untreated silica.
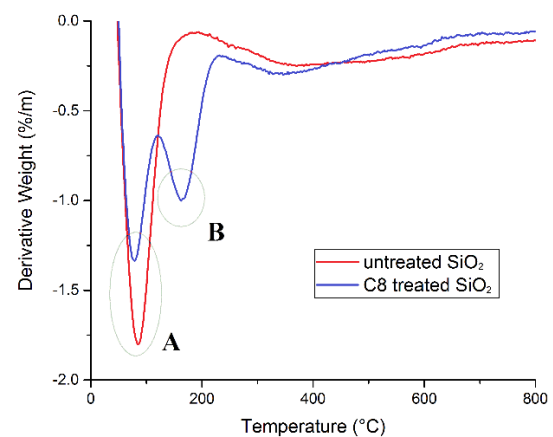

FIG. 1. TGA derivative result of untreated and C8-treated SiO_2 particles with dichloromethane (DCM). Reproduced by permission of the Institution of Engineering & Technology from ref [15].

Table 1. Particle information

Type	Size (*nm*)	Structure	Shape
SiO_2	10-20 (BET)	Crystalline	Spherical
BN	900(Average particle size) 200-500 (Crystal Size)	Hexagonal crystalline	Platelets

2.2. Experiment Set-up and Characterisation Methods

EVO® 50 scanning electron microscopy (SEM) was used to characterise the morphology of epoxy and its nanocomposites. The gun voltage was set to 15 kV with a working distance of 7-12 mm. All samples were coated with gold before the test by the Emitech K550X sputter coater at 25 mA for 3 min for each sample.

Thermo Gravimetric Analysis (TGA) was performed on Perkin-Elmer Pyris 1 thermogravimetric analyser. Samples were weighted as same as possible with the mass of around 5 mg and tested by measuring the weight loss under air gas flow of 20 ml min^{-1} at rate of 10 ℃·min^{-1} from 50 to 850 ℃. The surface treatment of SiO_2 particles was verified by TGA as well. The first peak A is caused by evaporation of dichloromethane (DCM), and the second peak B is believed due to loss of trimethoxy (octyl) chains on particle surfaces.

A power-compensated Perkin-Elmer DSC 7 was used with a nitrogen gas feed, controlled and finally being analyzed by Perkin-Elmer Pyris software. Samples used for testing are uniformly selected on films in each loading concentration of particles, and 5 pieces in total. The selected rate of temperature is 10 ℃·min^{-1} for all the measurements of DSC and temperature ranges from 50 ℃ to 150 ℃.

Table 2. Sample coding and loading concentrations. Reproduced by permission of the Institution of Engineering & Technology from ref [15].

Sample Code	Type of particles	Theoretical loading concentration (*wt%*)	Real loading concentration (*wt%*)
EP0	N/A	N/A	N/A
EPS05		0.5	0.751 ± 0.090
EPS1	untreated SiO_2	1	1.236 ± 0.081
EPS3		3	2.837 ± 0.021
EPS5		5	4.750 ± 0.078
EPST05		0.5	0.634 ± 0.096
EPST1	C8-treated SiO_2	1	1.110 ± 0.136
EPST3		3	2.551 ± 0.047
EPST5		5	4.468 ± 0.090
EPB05		0.5	0.713 ± 0.028
EPB1	hBN	1	0.967 ± 0.062
EPB3		3	3.211 ± 0.038
EPB5		5	5.161 ± 0.086

3. Results and Analysis

3.1. SEM Characterisation

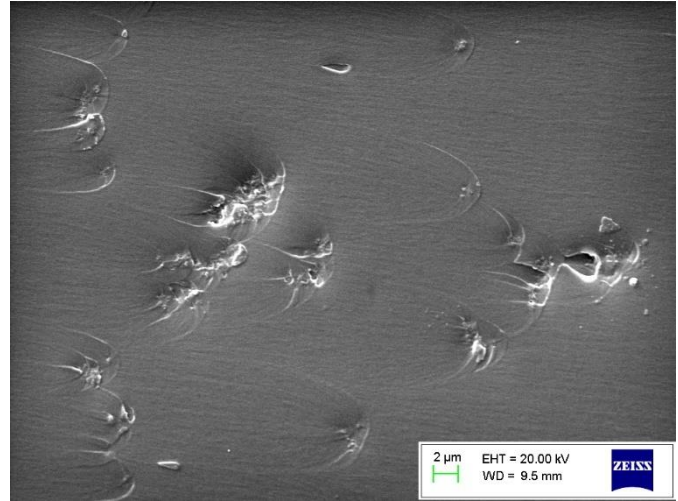The SEM images of EPS and EPST samples of 3 wt% and 5 wt% are shown in Fig. 2-5.

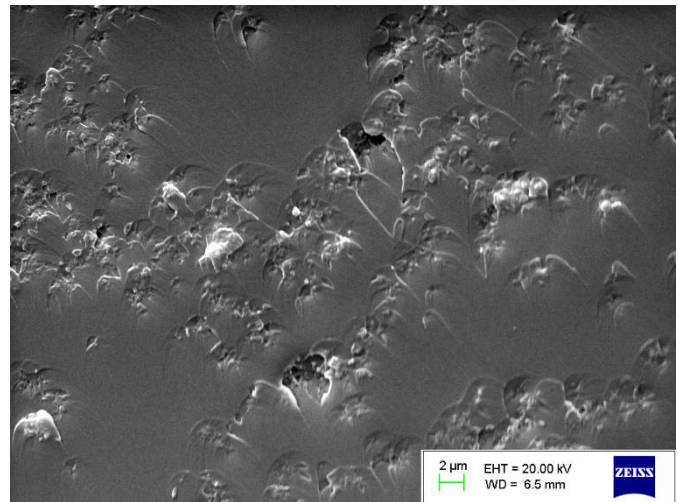FIG. 2. SEM image of untreated SiO_2 based epoxy nanocomposites, ×5000, 1 wt %.

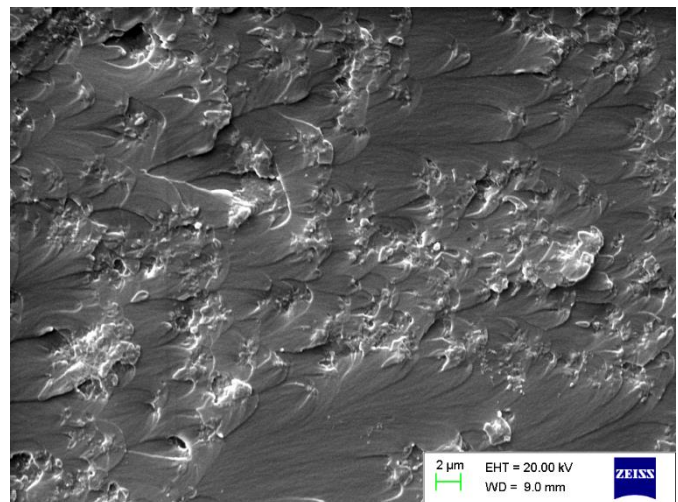FIG. 3. SEM image of untreated SiO_2 based epoxy nanocomposites, ×5000, 3 wt %.

FIG. 4. SEM image of untreated SiO_2 based epoxy nanocomposites, ×5000, 5 wt%.
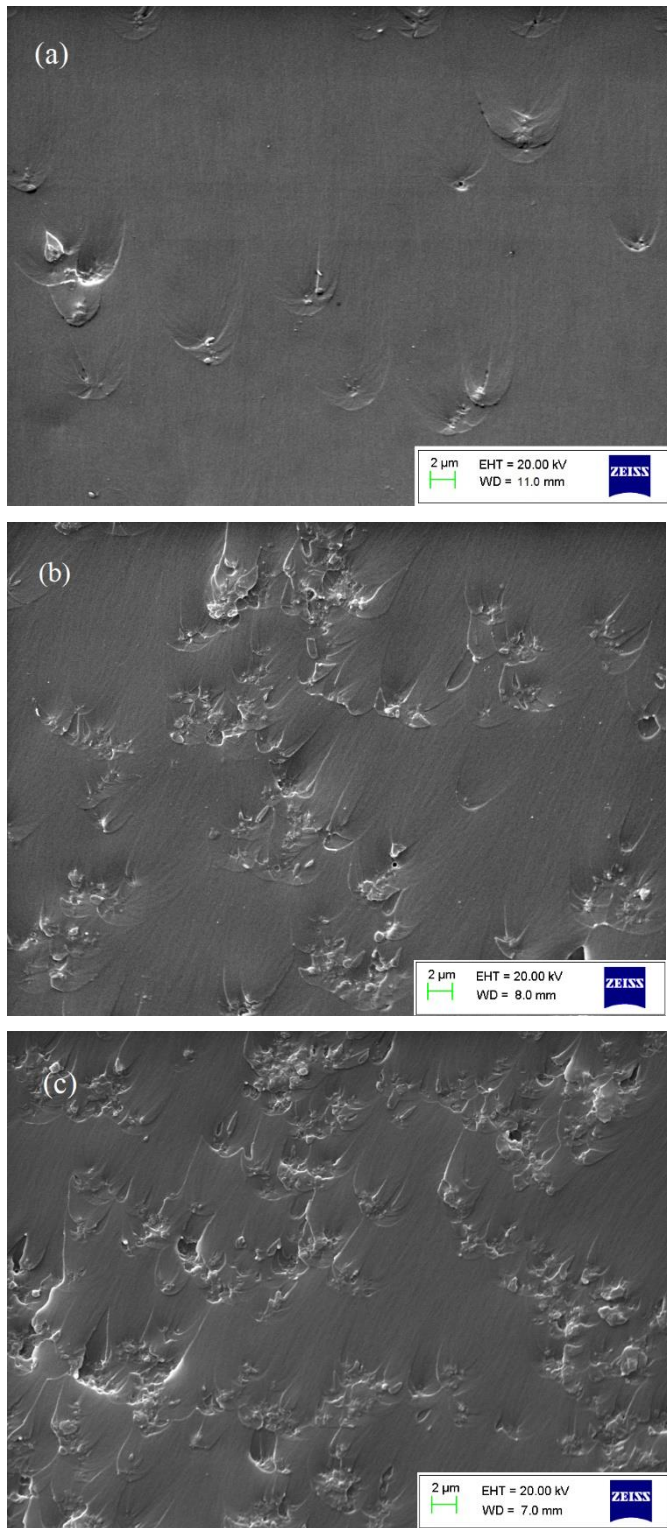
FIG. 5. SEM image of C8-treated SiO$_2$ based epoxy nanocomposites, ×5000: (a) 1 wt%; (b) 3 wt%; (c) 5 wt%.

It is noticed that the number of particles in EPS and EPST samples both increase with filler loading concentrations. In 3 wt% of EPS and EPST samples, obvious agglomerations of particles/aggregates have appeared and it seems that the fillers

have had a significant impact on the structure of the matrix, especially in EPS5 samples shown in Fig. 4.
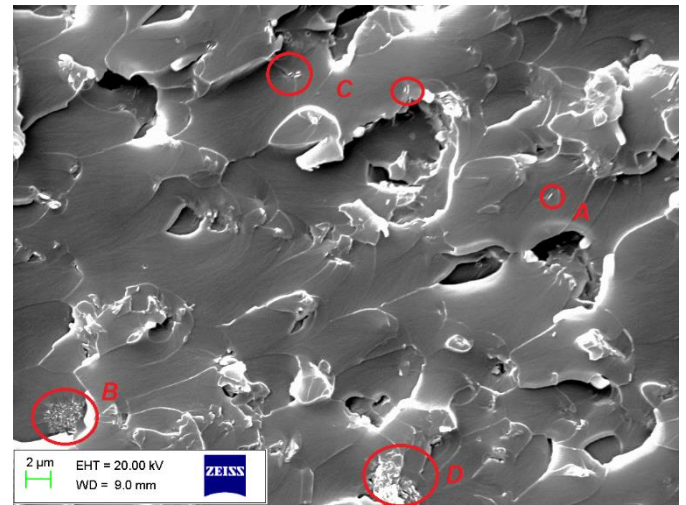

FIG. 6. SEM image of BN based epoxy nanocomposites, ×5000, 1 wt%.

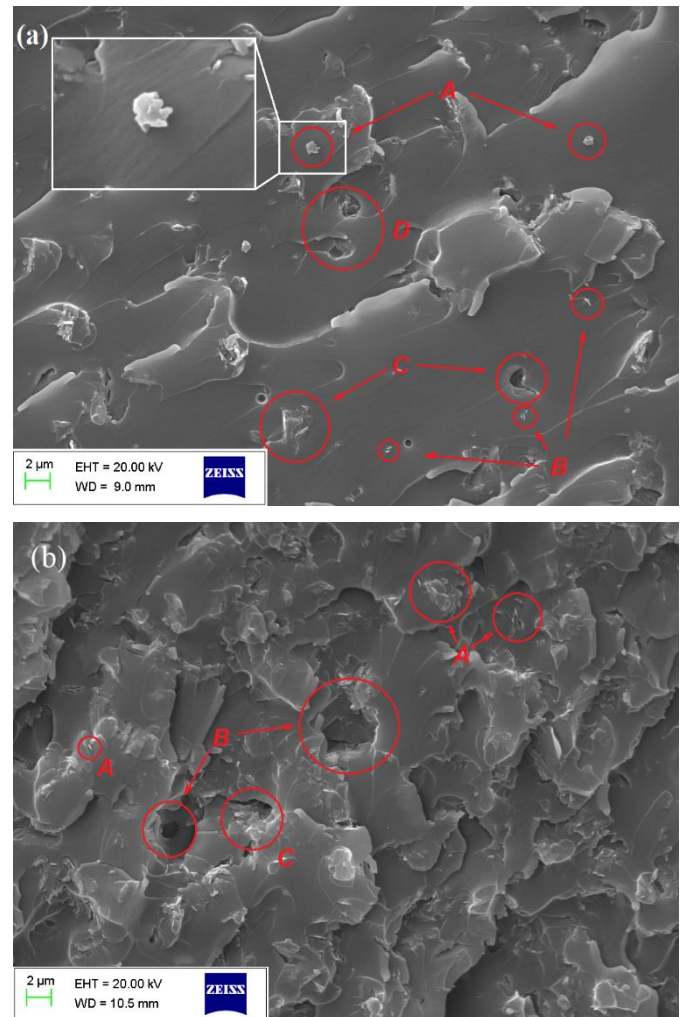
FIG. 7. SEM image of BN based epoxy nanocomposites, ×5000: (a) 1 wt%; (b) 3 wt%. Reproduced by permission of the Institution of Engineering & Technology from ref [15].

The more significant impact on the structure of the matrix morphology may lead to deteriorated properties in epoxy nanocomposites. Comparing EPS and EPST samples, it is easy to note that the surface treatment acts to reduce disturbance of the polymer matrix, this is especially clear for high filler concentrations of SiO_2 samples. EPST3 and EPST5 samples seem to show relatively better dispersion and distribution (shown in Fig. 5).
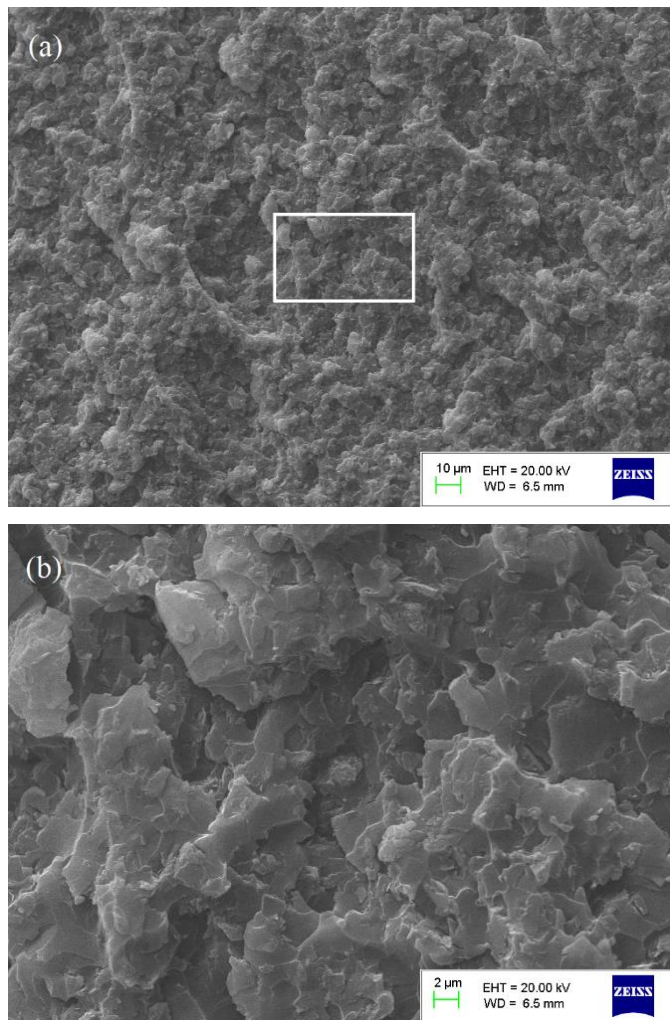

FIG. 8. SEM image of BN based epoxy nanocomposites, ×5000, 5 wt%: (a) ×1000; (b) Zooming into the square area in (a).

The SEM images of EPB samples are shown in Fig. 6-9. For this type of nanoparticles it can be concluded there are three distinct forms, which have also been observed in clay platelet-based nanocomposites [7]: First, due to the sonication process, particles can be exfoliated and solely dispersed in the matrix as shown in *Circle A* of Fig. 6 and Fig. 7(b), or loosely agglomerate together (see in *Circle B* of Fig. 6). Second, particles are also agglomerated as sphere-like aggregates as shown in *Circle A* of Fig. 7(a) and in the high magnification insets within Fig. 9. Third, some exfoliated particle plates could intercalate with the chains or their segments [7] as shown in *Circle C* of Fig. 6 and *Circle B* of Fig. 7(a) and

*Circle*s in Fig. 9. Moreover, the presence of hBN particles could lead to some stress concentration sites and initiation of cracks [16]. This type of feature is shown in *Circle D* of Fig. 7(a) and *Circle B* of Fig. 7(b). The cracking and disruption of the matrix become more severe in samples of higher filler loading. It is obvious that hBN particles have a much more noticeable impact on the morphology of base material than SiO_2 nanoparticles and tend to produce a layered structure in the matrix as shown *Circle D* of Fig. 6, *Circle C* of Fig. 7(b) and Fig. 8, and become more obvious with an increase of filler loadings.
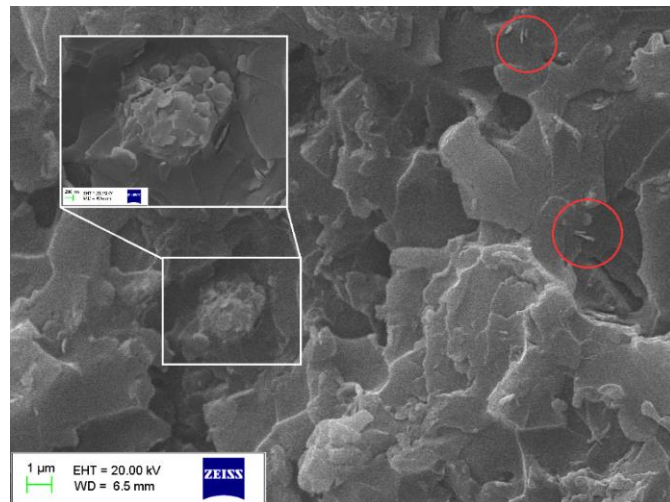

FIG. 9. SEM image of BN based epoxy nanocomposites, ×10000, 5 wt%, (inset, ×50000).

3.2. TGA Experiment

The purpose of the study in this section is to investigate the influence of nanoparticles on the thermal stability of epoxy composites. Normally, two temperature indexes are used to clarify the thermal stability: one is initial decomposition temperature (IDT) T_{IDT} which indicates the 5% weight loss of total mass, another is the maximum rate loss temperature T_{max} [5, 8, 17]. Those most representative results of EP0, EPS, EPST and EPB samples are shown in Fig. 10-12 and Fig. 14-16. In addition, two indexes are concluded in Table 3 and compared in Fig. 13 and Fig. 17.

As shown in Fig. 10 and 11, the initial decomposition temperature in EPS and EPST samples increase when compared to EP0, which is reportedly due to the filled silica restricting the mobility of polymer chains and acting as flame retardants for polymers [8, 18, 19]. The filled silica particles near the surface would form a layer to protect the materials from oxidizing [8, 20]. For EPS, there is a lower value in 0.5 wt% samples than the EP0 and may result from a lower cross-linking degree [21].

With the increase in filler loadings, the surface protective effect becomes dominant again. EPST shows similar increasing trends of T_{IDT}, however, results in most filler

loadings are higher than the EPS samples. This phenomenon may be caused by the hydroxyl groups being left on silica particles in EPS samples that will lead to the formation of hydrogen bonds, then low cross-linking density at the interface and further lowering the T_{IDT}.
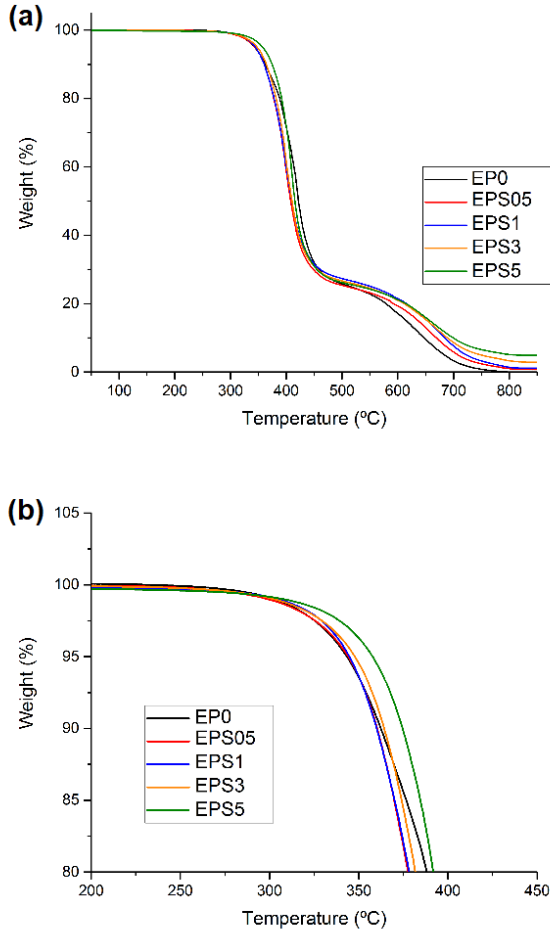

FIG. 10. TGA traces of EP0 and EPS: (a) whole; (b) zooming in to initial decomposition temperature range.

In EPB samples, as mentioned in section 3.1, hBN particles could have a significant impact on the base material and lead to very low curing density. Such low curing density will create large numbers of short chains. As short chains are more thermally stable than longer ones which should exist more in EPS and EPST, T_{IDT} of EPB samples is higher than that of silica nanocomposites at 0.5 and 1 wt% and EP0. However, T_{IDT} of EPB decreases with the growth of filler loadings. This should be due to the much higher thermal conductivity of hBN when compared to silica particles as shown in Fig. 13, which are 20-400 $W \cdot m^{-1} K^{-1}$ [22] and 1.4 $W \cdot m^{-1} K^{-1}$ [23]. The higher thermal conductivity of nanocomposites in high loadings results in much more thermal energy transported into bulk and enhances the decomposition of polymers, despite the

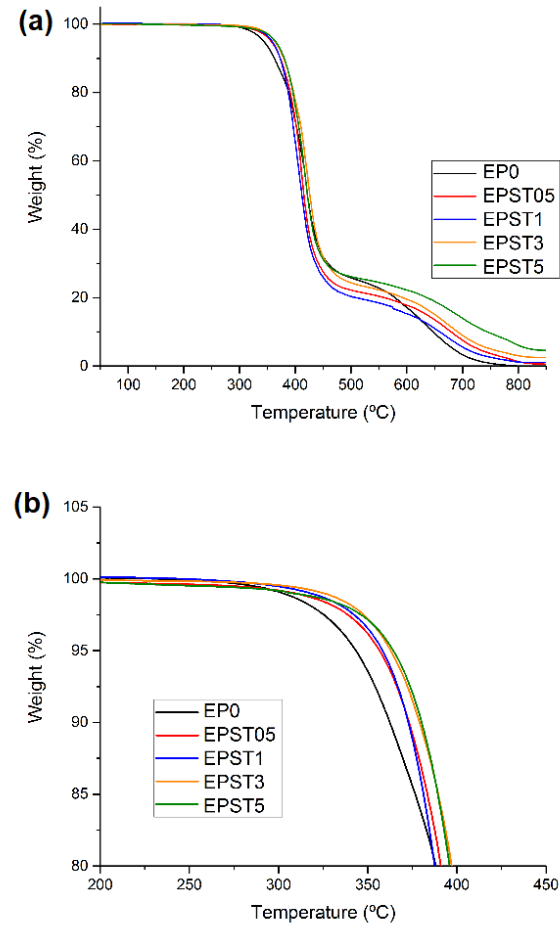protective effect of particles near the materials' surface still working.

FIG. 11. TGA traces of EP0 and EPST: (a) whole; (b) zooming in to initial decomposition temperature range.

As shown in Fig. 17, because most surface protective layers have been removed due to longtime decomposition, T_{max} reflects the thermal stability of composites in bulk. Owing to the lower cross-linking density resulting from adding particles, all nanocomposites show lower T_{max} than EP0 [5, 8], whereas EPB05 shows higher value due to the higher stability of short chains. For EPS and EPST, the increasing T_{max} in high loadings should be caused by the formation of carbonaceous-silicate char that hinders/slows the oxidisation of bulks [6]. In addition, the difference between them shares the same mechanism in that of T_{IDT}. Most T_{IDT} and T_{max} results of EPB samples are little higher than EPS samples, which may indicate that the thermal stability in the high temperature of epoxy BN nanocomposites is better than untreated silica samples. However, the stability of EPB becomes worse while increasing the filler loadings.
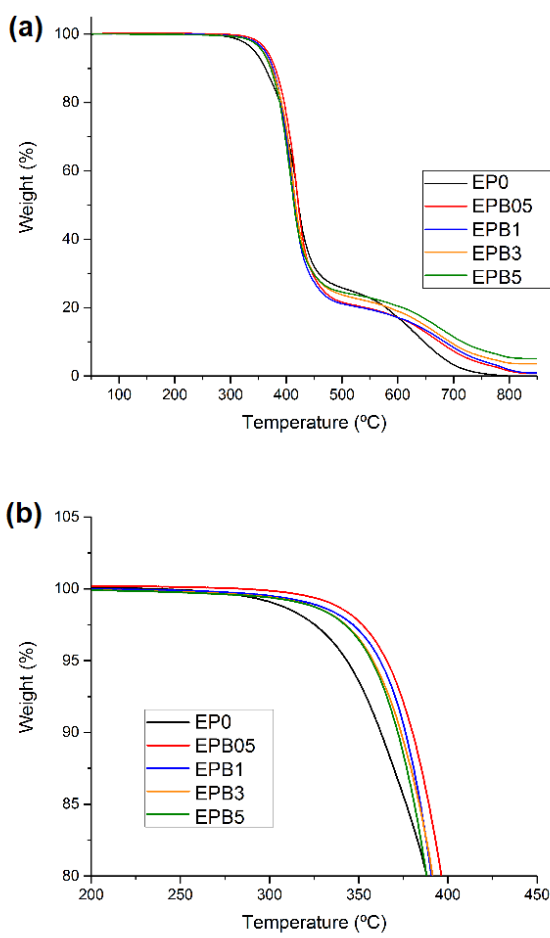
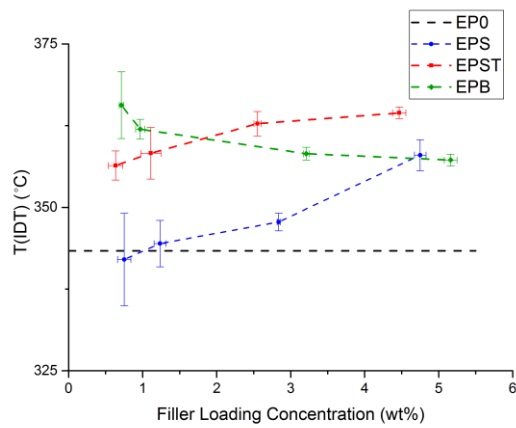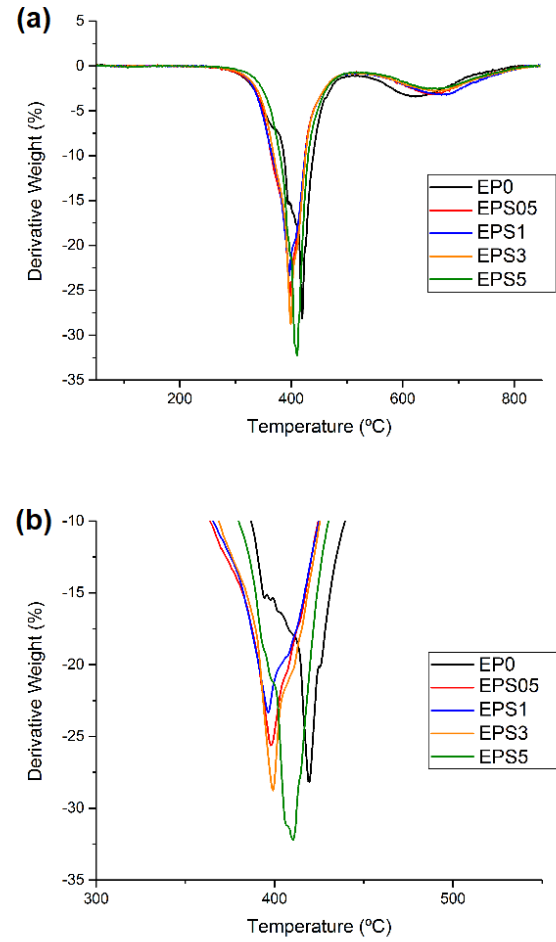FIG. 12. TGA traces of EP0 and EPB: (a) whole; (b) zooming in to initial decomposition temperature range.

FIG. 14. Derivative traces of EP0 and EPS: (a) whole; (b) zooming in to the temperature range at the maximum rate of decomposition.

Table 3. T_{IDT} and T_{max} of epoxy and its nanocomposites

Sample Code	T_{IDT} (ºC)	T_{max} (ºC)
EP0	343.35 ± 2.06	419.63 ± 3.58
EPS05	342.02 ± 7.07	397.87 ± 3.12
EPS1	344.46 ± 3.55	396.51 ± 2.77
EPS3	347.77 ± 1.36	399.18 ± 2.62
EPS5	357.99 ± 2.37	410.55 ± 3.27
EPST05	356.41 ± 2.22	409.30 ± 3.87
EPST1	358.28 ± 3.95	408.71 ± 1.63
EPST3	362.80 ± 1.87	420.99 ± 2.24
EPST5	364.45 ± 0.87	420.37 ± 2.78
EPB05	365.63 ± 5.11	421.31 ± 4.35
EPB1	361.96 ± 1.50	417.28 ± 1.34
EPB3	358.21 ± 0.98	410.27 ± 1.44
EPB5	357.25 ± 0.90	406.78 ± 1.06

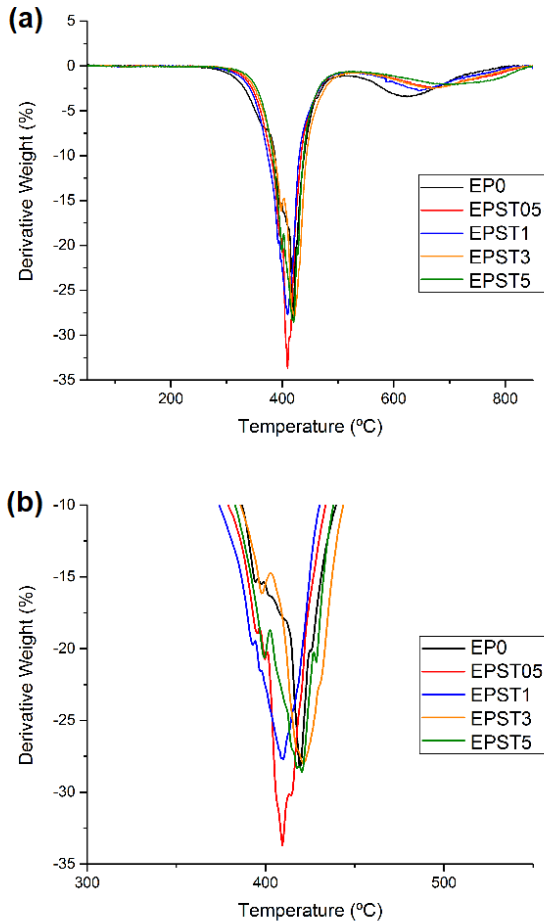FIG. 13. Comparison of T_{IDT} of EP0, EPS, EPST and EPB samples in different loading concentrations.

FIG. 15. Derivative traces of EP0 and EPST: (a) whole; (b) zooming in to the temperature range at the maximum rate of decomposition.

3.3. DSC Experiment

The DSC traces and glass transition temperature of EP0, EPS, EPST and EPB samples are shown and summarized in Fig. 18-21. The most representative curves of each loading, which means the glass transition temperatures of them are the closest ones to the average values of each-five-test, are plotted in Fig. 18(a), 19(a) and 20. The average T_g of each five-piece of EP0, EPS, EPST and EPB samples are shown in Fig. 18(b), 19(b) and 21.

The glass transition temperature of a polymer system depends on various factors, including changes of the molecular weight, chain segment mobility, density of crosslinking, and the amount of reaction residue acting as a plasticiser [24]. In this project, the ingredients and curing conditions of the nanocomposites were the same for all the samples. Thus, it is possible to make sure the changes in T_g are mainly due to the different loading concentrations, properties of the fillers and their influences upon the base material. It is obvious that the T_g of epoxy nanocomposites is overall lower

than that of EP0 and decreases with the growth of filler loading concentrations, though EPB5 shows an enhancement of T_g. This phenomenon should be, first, due to the lower cross-linking density of epoxy nanocomposites [5, 9, 25].
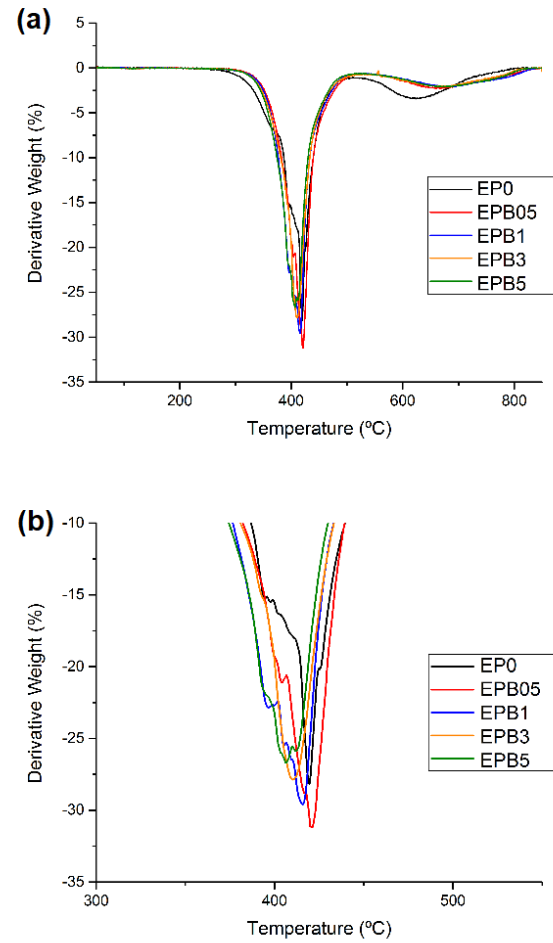

FIG. 16. Derivative traces of EP0 and EPB: (a) whole; (b) zooming in to the temperature range at the maximum rate of decomposition.
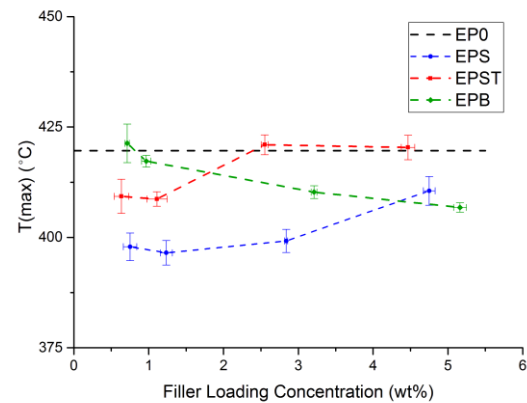

FIG. 17. Comparison of T_{max} of EP0, EPS, EPST and EPB samples in different loading concentrations.
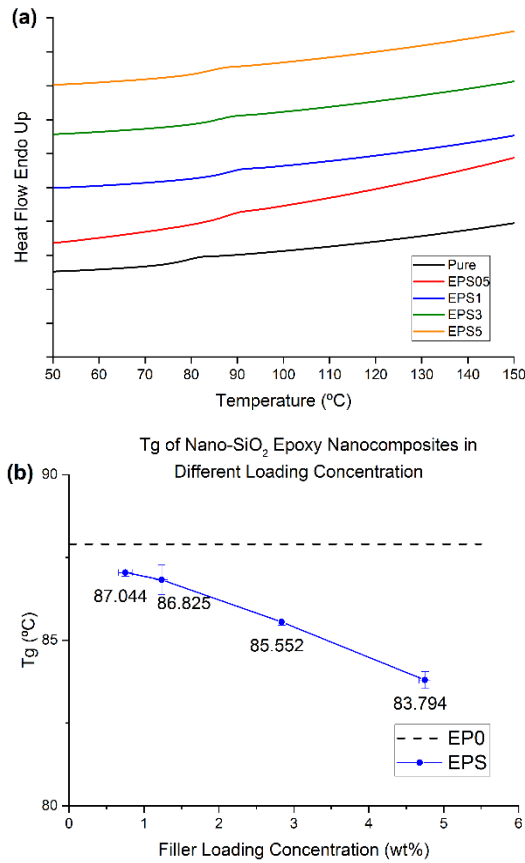
8

FIG. 18. (a) DSC traces of EP0 and EPS samples; (b) Average T_g of EPS samples, in different filler loading concentrations.

FIG. 19. (a) DSC traces of EP0 and EPST samples; (b) Average T_g of EPST samples, in different filler loading concentrations.

Second, the surface characteristics of nanoparticles and the interfacial region between the polymer matrix and nanofillers can be used to explain the behaviours of T_g. Early studies indicated that the interfacial region was the most critical factor that influenced the T_g of polymer nanocomposites by *Starr* et al. [26, 27]. *Santanu* and *Thomas* then introduced the Dual Layer Model to explain the behaviours of T_g [26, 27]. In this model, the interfacial region around the nanofillers is divided into a tightly and loosely bound layer. The tightly bound region is the inner layer and it is tightly bound between nanoparticles and polymer chains by weak hydrogen bonds and thus limits the movements of the chains, which could increase the T_g. However, as the surface treatment of EPST samples is not suitable, there is no tightly bound chain and this results in higher mobility of chains in the interfacial areas. Thus, the T_g of EPST samples is lower than that of EPS. With the increase in filler loadings, the volume fraction of the interfacial area between the T_g matrix and particles increases significantly, especially the loosely bound layer where free volumes are more likely to locate, and this leads to the increase in free volume and the further reduction of T_g [27-29]. This has also been observed in [30, 31].
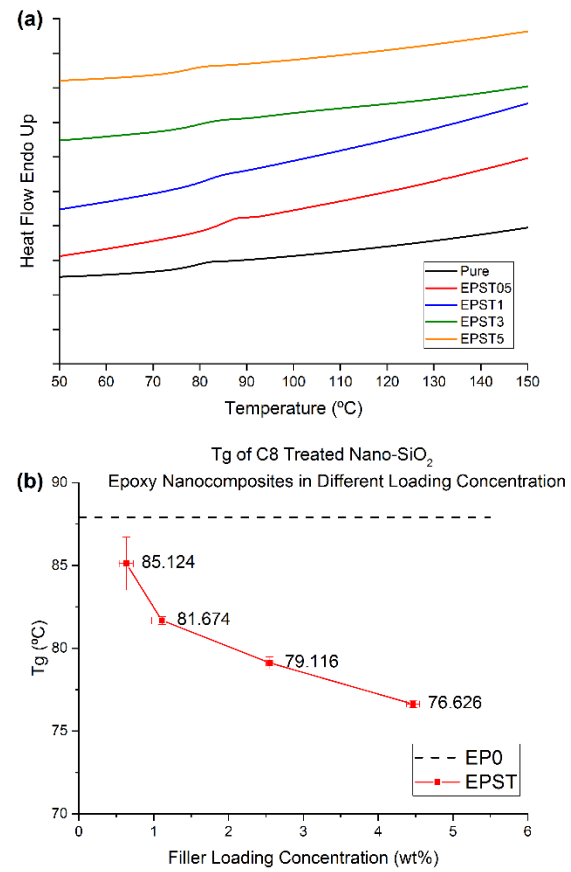

FIG. 20. DSC traces of EP0 and EPB samples.

Regarding the EPB samples, the obvious lower value of T_g than pure and silica-based composites should be mainly due to the significant low cross-linking density of curing, which should become worse with the increase in filler loadings. Moreover, the higher thermal conductivity of hBN could play a role as well. However, it is noticed there is a smaller reduction of T_g in EPB3 and even increase in EPB5. This

should be due to a mix of the exfoliated and intercalated macroscopic layer structures of hBN-based nanocomposites [32-34] as shown in Fig. 22 which would impair the mobility of chain segments in the vicinity of particles, and thus increase the glass transition temperature [25, 35].
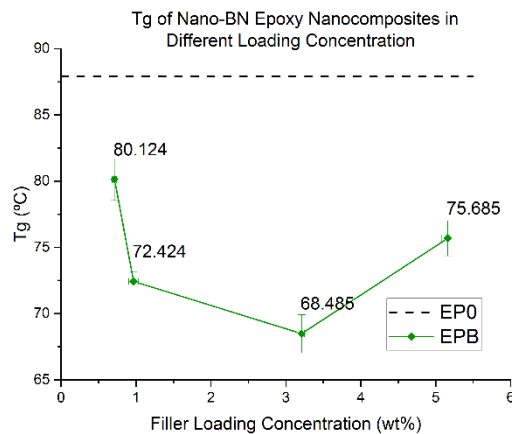

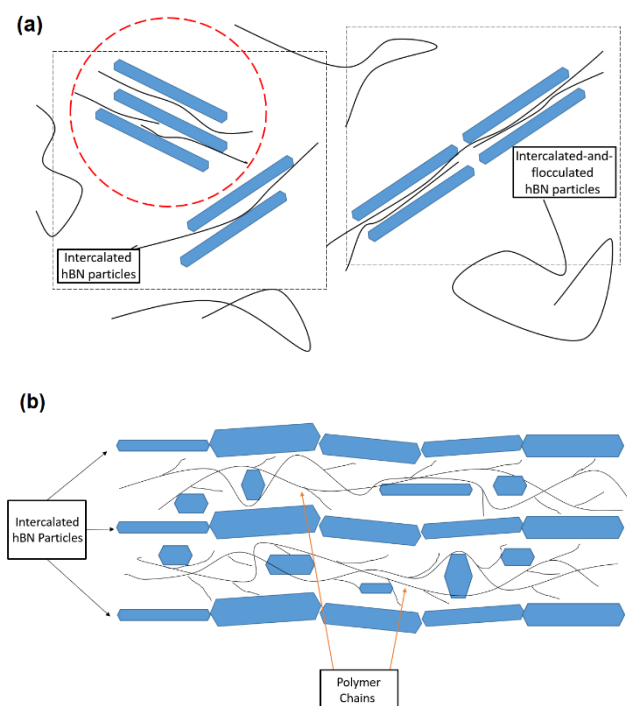FIG. 21. Average T_g of EPB samples, in different filler loading concentrations.

FIG. 22. (a) Illustration of exfoliated and intercalated macroscopic layer structures of hBN-based epoxy nanocomposites; (b) structure of circled area in (a).

4. Conclusions

According to the present work, the chemical structures and thermal properties of epoxy and its nanocomposites were investigated by TGA and DSC measurements, and the following conclusions can be made:

- The presence of nano-SiO$_2$ and hBN particles both led to the decrease in cross-linking density during curing of epoxy resins and further resulted in worse thermal stability than pure samples. However, particles acted as flame retardants for polymers and postponed the initiation of decomposition by hindering/slowing the oxidisation.

- When compared within two SiO$_2$-based samples, surface treatment modified the cross-linking density in the interfacial areas by getting rid of some surface groups, like hydroxyl groups found in EPS samples, but unsuitable surface treatment led to the higher mobility of chain segments at the interface and thus the reduction of T_g in EPST samples.

- The morphology of EPB samples had a significant impact on its thermal properties: in TGA measurement, shorter chains resulted in improved performance when decomposing, while in the DSC measurement, exfoliated and intercalated macroscopic layer structures of hBN-based nanocomposites, which was observed in morphology characterisation by SEM, restricted the mobility of chain segments in the vicinity of particles and led to the increase in T_g in samples with higher filler loadings.

- The cross-linking density of samples should mainly affect the results of TGA, whereas the mobility of chain segments played the main role in influencing the glass transition temperature of polymer composites.

References

[1]   Hedrick J L, Yilgör I, Wilkes G L, and McGrath J E 1985 *Polymer Bulletin* **13** 201-208

[2]   Gao C 2001 *Journal of Jiangsu University of Science and Technology* **22** 63-70

[3]   Dakin T W 1974 *IEEE Transactions on Electrical Insulation* **EI-9** 121-128

[4]   Andritsch T, Delft University of Technology, 2010.

[5]   Gu A and Liang G 2003 *Polymer Degradation and Stability* **80** 383-391

[6]   Modesti M, Lorenzetti A, Bon D, and Besco S 2006 *Polymer Degradation and Stability* **91** 672-680

[7]   Kumar A P, Depan D, Tomer N S, and Singh R P 2009 *Progress in polymer science* **34** 479-515

[8]   Tarrío-Saavedra J, López-Beceiro J, Naya S, and Artiaga R 2008 *Polymer Degradation and Stability* **93** 2133-2137

[9]   Luo Q, Li Y, Pan L, Song L, Wu L, and Lu S 2016 *Journal of materials science* **51** 8888-8899

[10]   Gu J, Zhang Q, Dang J, and Xie C 2012 *Polymers for Advanced Technologies* **23** 1025-1028

[11]   Yung K and Liem H 2007 *Journal of Applied Polymer Science* **106** 3587-3591

[12]   Yu J, Huang X, Wu C, Wu X, Wang G, and Jiang P 2012 *Polymer* **53** 471-480

[13]   Lau K Y, 2013, PhD Thesis, University of Southampton.

[14]   Reading M, Xu Z, Vaughan A S, and Lewin P L 2011 in *Electrical Insulation Conference (EIC)* 493-497.

[15]   Qiang D, Wang Y , Chen G and Andritsch T 2018 IET Nanodielectrics **1** 48-59.

[16]   Saha M *et al.* 2015 *Composite Interfaces* **22** 611-627

[17]   Liu Y-L, Wei W-L, Hsu K-Y, and Ho W-H 2004
          Thermochimica Acta **412** 139-147
[18]   Macan J, Brnardić I, Orlić S, Ivanković H, and Ivanković
          M 2006 *Polymer Degradation and Stability* **91** 122-127
[19]   Park S-J, Kim H-C, Lee H-I, and Suh D-H 2001
          Macromolecules **34** 7573-7575
[20]   Liu Y-L, Hsu C-Y, Wei W-L, and Jeng R-J 2003 *Polymer*
          44 5159-5167
[21]   Preghenella M, Pegoretti A, and Migliaresi C 2005
          Polymer **46** 12065-12072
[22]   Jin-Cheng Z *et al.* 2016 *2D Materials* **3** 011004
[23]   Lines M. 2001. *Silica - Silicon Dioxide (SiO$_2$)*. Available
          at: https://www.azom.com/article.aspx?ArticleID=1114
[24]   Sun Y, Zhang Z, Moon K-S, and Wong C P 2004 *Journal
          of Polymer Science Part B: Polymer Physics* **42** 3849-
          3858
[25]   Corcione C E and Frigione M 2012 *Materials* **5** 2960-
          2980
[26]   Starr F W, Schrøder T B, and Glotzer S C 2001 *Physical
          Review E* **64** 021802
[27]   Lewis T J in *Proceedings of the 2004 IEEE International
          Conference on Solid Dielectrics (ICSD)* **2** 792-795.
[28]   Ash B J, Schadler L S, and Siegel R W 2002 *Materials
          Letters* **55** 83-87
[29]   Tsagaropoulos G and Eisenberg A 1995 *Macromolecules*
          28 6067-6077
[30]   Mayes A M 2005 *Nature Materials* **4** 651
[31]   Nelson J K and Hu Y in *Proceedings of the 2004 IEEE
          International Conference on Solid Dielectrics (ICSD)* **2**
          832-835.
[32]   Lin Z, Liu Y, Moon K-s, and Wong C-P in *Electronic
          Components and Technology Conference (ECTC), 2013
          IEEE 63rd* 1692-1696.
[33]   Lin Z, Liu Y, Raghavan S, Moon K-s, Sitaraman S K, and
          Wong C-p 2013 *ACS applied materials & interfaces* **5**
          7633-7640
[34]   Shen H, Cai C, Guo J, Qian Z, Zhao N, and Xu J 2016
          RSC Advances **6** 16489-16494
[35]   Esposito Corcione C, Mensitieri G, and Maffezzoli A
          2009 *Polymer Engineering & Science* **49** 1708-1718